Chinese Chemical Letters 36 (2025) 110316

Contents lists available at ScienceDirect

Chinese Chemical Letters

journal homepage: www.elsevier.com/locate/cclet

Enhanced venetoclax delivery using L-phenylalanine nanocarriers in acute myeloid leukemia treatment

Liangyu Zhang[a,b,1], Lei Lei[c,1], Zhuangzhuang Zhao[d,1], Guizhi Yang[b], Kaitao Wang[a,b], Liying Wang[a], Ningxin Zhang[e], Yanjia Ai[e], Xinqing Ma[b], Guannan Liu[b], Meng Zhao[a,b,f,*], Jun Wu[a,g,h,*], Dongjun Lin[a,*], Chun Chen[i,*]

[a] Department of Hematology, The Seventh Affiliated Hospital, Zhongshan School of Medicine, Sun Yat-sen University, Shenzhen 518107, China
[b] Key Laboratory of Stem Cells and Tissue Engineering (Ministry of Education), Zhongshan School of Medicine, Sun Yat-sen University, Guangzhou 510080, China
[c] Department of Nephrology, Center of Kidney and Urology, The Seventh Affiliated Hospital, Zhongshan School of Medicine, Sun Yat-sen University, Shenzhen 518107, China
[d] Changzhi Medical College, Changzhi 046000, China
[e] Department of Hematology, Nanfang Hospital, Southern Medical University, Guangzhou 510515, China
[f] Advanced Medical Technology Center, The First Affiliated Hospital, Zhongshan School of Medicine, Sun Yat-sen University, Guangzhou 510080, China
[g] Bioscience and Biomedical Engineering Thrust, The Hong Kong University of Science and Technology (Guangzhou), Guangzhou 511400, China
[h] Division of Life Science, The Hong Kong University of Science and Technology, Hong Kong SAR 999077, China
[i] Department of Pediatrics, The Seventh Affiliated Hospital, Zhongshan School of Medicine, Sun Yat-sen University, Shenzhen 518107, China

ARTICLE INFO

Article history:
Received 11 June 2024
Revised 3 August 2024
Accepted 5 August 2024
Available online 5 August 2024

Keywords:
Acute myeloid leukemia
Venetoclax
L-Phenylalanine
Chemoresistance
Nanoparticles

ABSTRACT

Venetoclax (Vene), a BCL-2 inhibitor, is widely used as a chemotherapeutic drug in acute myeloid leukemia (AML). However, its treatment specificity for leukemia cells is limited, often leading to side effects and treatment resistance. In this study, we utilized L-phenylalanine as an efficient nanocarrier to enhance the delivery of Vene, forming the complex Vene@8P6. This complex was then applied to AML mouse models and human AML cell lines. The *in vitro* analysis showed that THP-1 and HL60 cells rapidly absorbed the Vene@8P6 nanoparticles. This absorption resulted in severe DNA damage, increased reactive oxygen species (ROS) production, elevated apoptosis rates, and decreased cell proliferation compared to the administration of Vene alone. *In vivo* studies demonstrated that Vene@8P6 more efficiently targeted leukemia cells than normal hematopoietic cells within the bone marrow and other major organs in AML mice, as evidenced by bioluminescence imaging and flow cytometry analysis. Furthermore, Vene@8P6 treatment resulted in reduced drug side effects and improved therapeutic efficacy in AML mice. Overall, Vene@8P6 represents a novel and efficient therapeutic agent for AML, offering enhanced leukemia target specificity, reduced side effects, and improved treatment outcomes.

Acute myeloid leukemia (AML) is a highly heterogeneous malignant clonal disease derived from hematopoietic stem and progenitor cells, characterized by myeloid cells over amplification and hematopoietic dysfunction [1-3]. As one of common hematological malignancy, the morbidity rate accounts for approximate 80% of adult acute leukemia [4]. Extensive differences still exist among patients in disease course and prognosis despite of continued progress made on treatment. The percentage of AML patients administrated with chemotherapy who survive over 5 years after diagnosis is less than 40% [5-8].

Venetoclax (Vene), the inhibitor of B-cell lymphoma-2 (BCL-2), directly binds to BCL-2 protein, then releases pro-apoptotic proteins Bim and Bax, resulting in mitochondrial outer membrane permeability variety and tumor apoptosis [9-12]. Vene combined with other chemotherapy agents has been a common clinical treatment for leukemia [13-15]. The combination with azacitidine efficiently decreased the anti-apoptotic protein myeloid cell leukemia-1 (MCL-1), interfered with the energy metabolism and functioned synergistically on leukemia stem cells [16-18]. Besides, Vene combined with Bromodomain and extra-terminal domain (BET) inhibitors and Fms-like tyrosine kinase 3 (FLT-3) inhibitors syner-

* Corresponding authors.
E-mail addresses: zhaom38@mail.sysu.edu.cn (M. Zhao), junwuhkust@ust.hk (J. Wu), lindongjun0168@163.com (D. Lin), chenchun@mail.sysu.edu.cn (C. Chen).
[1] These authors contributed equally to this work.

https://doi.org/10.1016/j.cclet.2024.110316
1001-8417/

gistically enhanced the anti-leukemia activity [19,20]. However, the administration of Vene exists an extend of severe myeloablation side effects, poorly targets leukemia cells, and damage normal blood cells, thus causing a series of body reactions, including thrombocytopenia, neutropenia, fever, anemia, leukopenia, *etc.* [21-23].

Tumor targeting based on tumor metabolic characteristics has been widely applied [24,25]. For instance, redox responsive polymeric nanoparticles and cancer cell membrane camouflaged biomimetic nanogel designed newly are respectively applied to the treatment of prostate cancer and tumor inhibition [26,27]. Besides, an increasing application of cancer treatment is based on nano technology platform, including the pH-responsive theranostic nanotechnology in the magnetic resonance imaging for cancer therapy [28]. Sun *et al.* developed MSN-Fe-CAuNC-DOX@HA nanosystem (MFADH), which presented obvious anti-tumor effects. Hyaluronic acid (HA), with characteristics of biocompatibility and precious tumor targeting, forms a coat that dissolves, allowing cationic bovine serum albumin-protected, doxorubicin-loaded gold nanoclusters (CAuNC-DOX) to be released and penetrate the tumor [29]. In our previous study, we verified that amino acid metabolism enabled to regulate immunity and cancer, and thus developed an L-phenylalanine based metabolic reprogramming immune surveillance activation nanomedicine [30,31]. The nanodrug 8P6 loaded with DOX precisely targeted T cell acute lymphoblastic leukemia (T-ALL) and extremely reduce the side effects of chemotherapy agents but maintained normal hematopoietic function stable [31]. However, the role of 8P6 in AML is still indistinct. Therefore, in this experiment, Vene-loaded 8P6 nanoparticles (Vene@8P6 NPs) were applied to human leukemia cell lines and mouse AML models.

The 8P6 polymer, a biodegradable L-phenylalanine-based poly(ester amide), was demonstrated great potential in drug delivery [32]. In this study, we utilized 8P6 polymer as a nanocarrier to deliver Vene, aiming to enhance its therapeutic efficacy against leukemia. Therefore, we synthesized 8P6 following the protocols described in a previous study [33]. Details are shown in Supporting information. Both 8P6 nanoparticles (8P6 NPs) and Vene@8P6 showed a narrow size distribution and spherical morphology (Figs. 1A–D). Compared with blank NPs, Vene@8P6 exhibited a slightly increased size (92.2 nm) and an enhanced negative zeta potential (−48.8 mV). Additionally, Vene@8P6 demonstrated an ultra-high drug loading efficiency (96.1%) and comparable drug loading capacity (19.4%) (Table 1). And stability tests indicated that the size of 8P6 NPs and Vene@8P6 changed slightly, suggesting good stability in physiological environments (Fig. 1E).

Table 1
Characterization of physicochemical properties of 8P6 NPs and Vene@8P6.

Sample	Size (nm)	PDI[a]	Zeta potential (mV)	DLC[b] (%)	DLE[c] (%)
8P6 NPs	84.3	0.17	−35.3	N/A	N/A
Vene@8P6 NPs	92.2	0.23	−48.8	19.4	96.1

[a] PDI: Polydispersity index.
[b] DLC: Drug loading capacity.
[c] DLE: Drug loading efficiency.

To detect the toxicity and influence of Vene@8P6 on mice, we collected other tissues for hematoxylin-eosin (HE) staining to examine whether 8P6 functioned on toxic side effects or body damage. In consistent with previous result [33], no obvious tissue damage represents on the heart, liver, spleen, lung, and kidney after Vene@8P6 treatment in mice (Fig. 1F). White blood cells (WBC), neutrophils (Neu), lymphocytes (Lym), red blood cells (RBC) and platelets (PLT) in peripheral blood of mice administered with 8P6 and Vene@8P6 presented no significant difference compared with the control group (Figs. 1G–K). Furthermore, we also examined the liver and kidney function, indicated by the alanine aminotransferase (ALT) and aspartate aminotransferase (AST), blood urea nitrogen (BUN) and creatinine (CREA), respectively (Figs. 1L–O). All the four indicators detected *via* peripheral blood plasma of mice, administered with a three-day consecutive injection of prescrip-

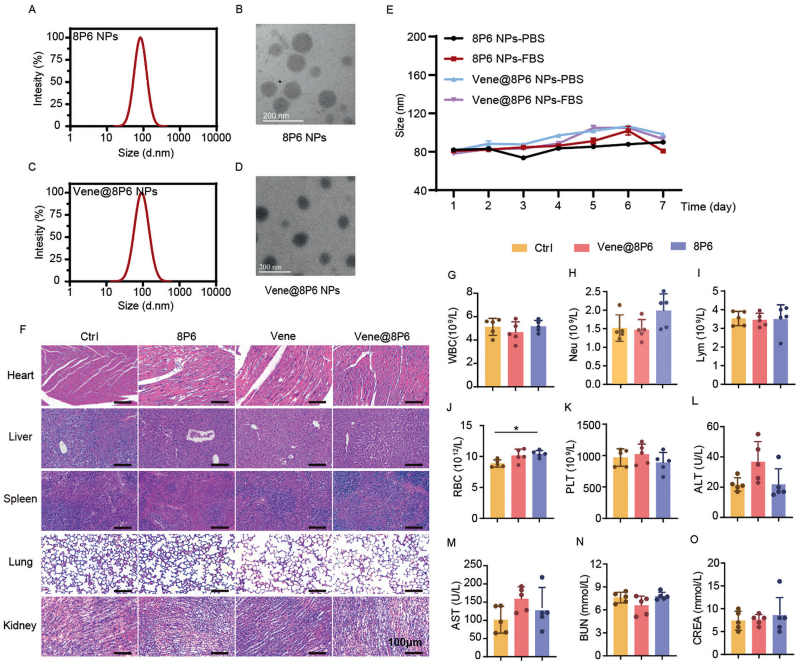

Fig. 1. Fabrication and characterization and *in vivo* biosafety of Vene@8P6. (A) Size distribution and (B) transmission electron microscopy (TEM) images of 8P6 NPs. Scale bar: 200 nm. (C) Size distribution and (D) TEM images of Vene@8P6. Scale bar: 200 nm. (E) Change in particle size. (F) Representative histopathological images of major organs from C57BL/6J mice with PBS, 8P6, Vene, Vene@8P6 for three consecutive days. Scale bar: 100 μm. The levels of WBC (G), Neu (H), Lym (I), RBC (J), PLT (K) of peripheral blood and ALT (L), AST (M), BUN (N) and CREA (O) in serum with indicated treatments were analyzed at 6 days after the last injection ($n = 5$ mice). $^{*}P < 0.05$. Data are presented as mean ± standard deviation (SD).

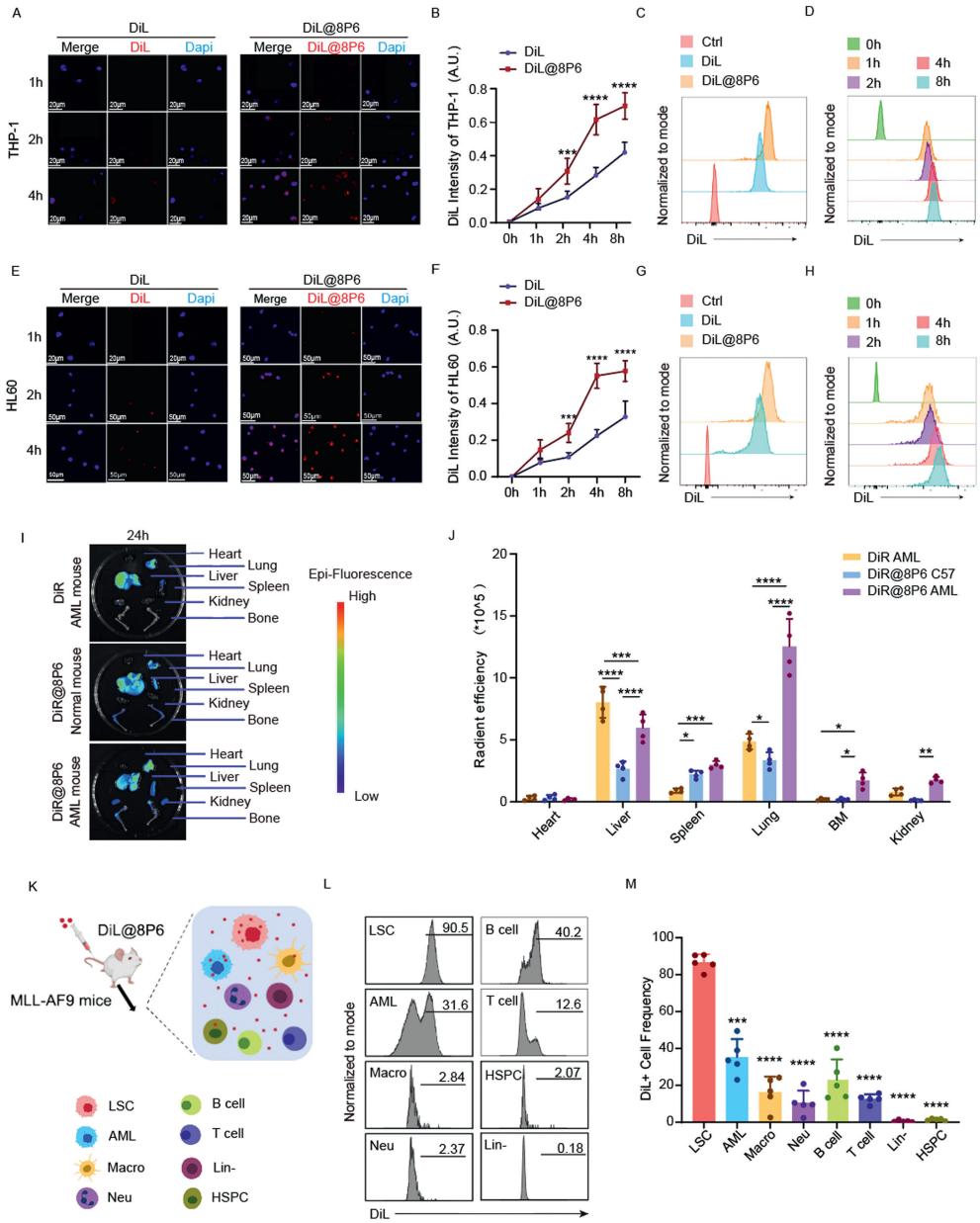

Fig. 2. 8P6 specifically targets AML cells and enhances cellular uptake efficiency. (A, B) Cell uptake of free DiL and DiL@8P6 in THP-1 leukemic cells. The representative images (A) and quantification of fluorescence intensity of DiL and DiL@8P6 (B). Scale bar: 20 μm. (C, D) The quantification of fluorescence intensity of Ctrl, DiL and DiL@8P6 at 4 h (C) and DiL@8P6 at 0, 1, 2, 4 and 8 h (D). (E, F) Cell uptake of free DiL and DiL@8P6 in THP-1 leukemic cells. The representative imaging (E) and quantification (F) of fluorescence intensity of DiL and DiL@8P6. Scale bar: 20 μm. (G, H) The quantification of fluorescence intensity of Ctrl, DiL and DiL@8P6 by FACS at 4 h (G) and DiL@8P6 at 0, 1, 2, 4, and 8 h (H). (I, J) *Ex vivo* fluorescence imaging (I) and quantification (J) of DiR intensity in indicated organs from AML and normal mice at 24 h after intravenous injection of free DiR or DiR@8P6 ($n = 5$ mice). (K) Scheme for quantifying DiL@8P6 uptake efficiency by leukemia cells and BM cells in MLL-AF9 mice. (L, M) The representative flow plots (L) and quantification (M) of DiL intensity in indicated cells from bone marrow of AML mice at 24 h after injection of DiL@8P6 ($n = 5$ mice). * $P < 0.05$, ** $P < 0.01$, *** $P < 0.001$, **** $P < 0.0001$. Data are presented as mean ± SD.

tion with 8P6, and not differ significantly. Our data consistently indicated that Vene@8P6 improved anti-leukemia effectiveness and reduced toxic side effects.

According to our previous exposition, L-phenylalanine-based polymer (8P6) was the main reason for the leukemic targeting, causing a higher cellular uptake than other hematopoietic cells and progenitors [31]. We further investigated the ability of 8P6 cellular uptake in AML cells *via* fluorescent dye *in vitro*. Meanwhile, we also assessed the cellular uptake of 8P6 with DiL as a fluorescent probe. Free DiL or DiL-loaded 8P6 (DiL@8P6) was intravenously injected into leukemic cells. In consistent as we speculated, DiL@8P6 manifested obviously and quickly than free dyes in both THP-1 cells and HL60 cells, which implied that 8P6 effectively targeted leukemic cells (Figs. 2A–H). Such observations were also verified in AML mice *in vivo* by injecting with DiR@8P6, which exhibited a much broader distribution than free DiR under bioluminescence monitoring. The construction of the MLL-AF9 AML murine model was followed the same as before [33]. To investigate the biodistribution of 8P6 *in vivo*, we adopted DiR was as a fluorescent probe for tracing 8P6 in the body. Fluorophore was obviously manifested in liver, spleen and lung of both C57 mice and AML mice (Fig. 2I). Intriguingly, DiR@8P6 was accumulated in most organs in AML mice (low level in the heart) and especially targeted bone marrow and spleen, which indicated that Vene could effec-

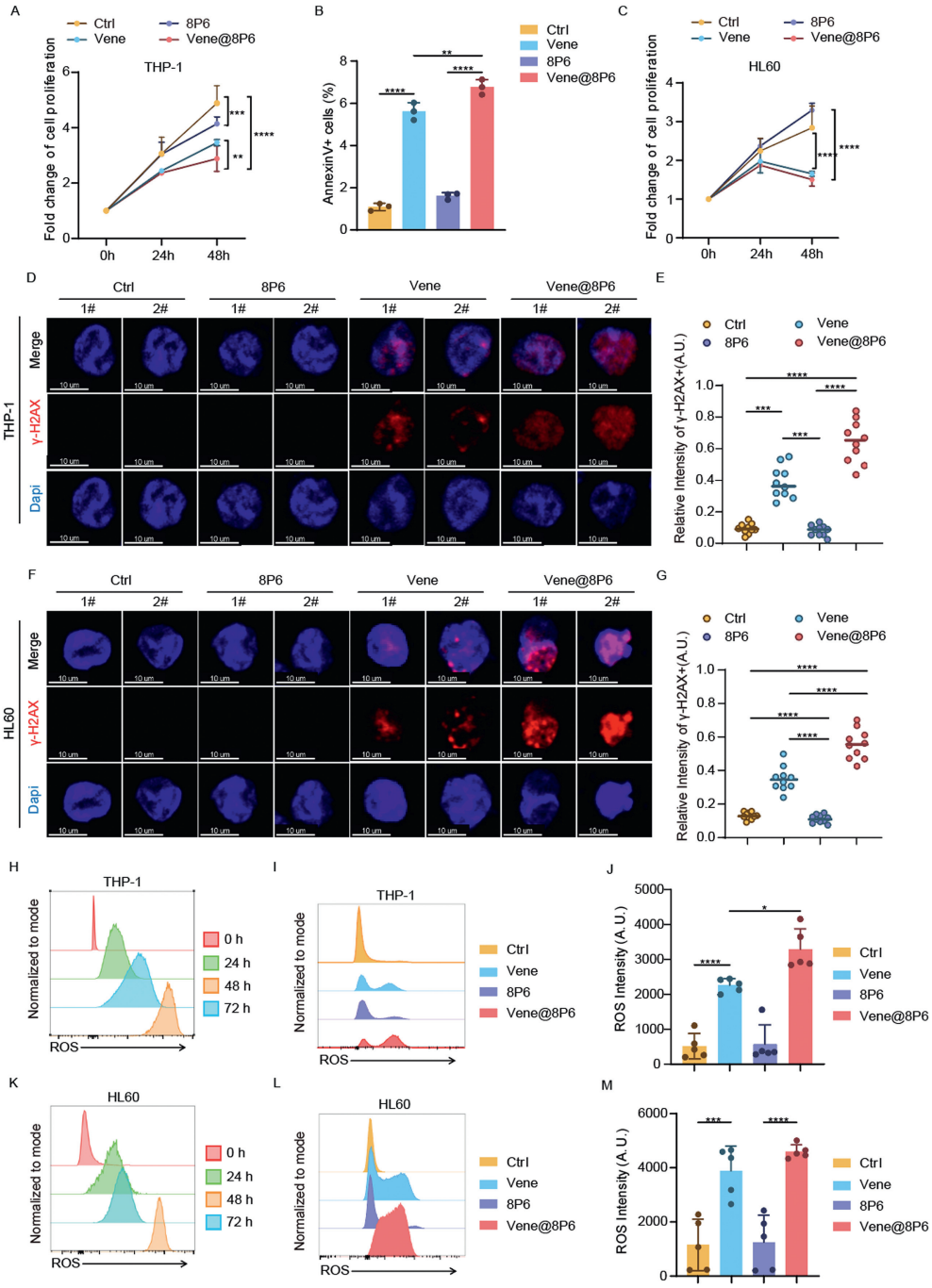

Fig. 3. Vene@8P6 enhanced ROS and induced DNA damage and apoptosis in AML cells. (A, B) Quantification of multiplication (A) and apoptotic (B) in THP-1 cells after treatment with PBS, Vene, 8P6, and Vene@8P6 at indicated time points. (C) Quantification of multiplication in HL60 cells after treatment with PBS, Vene, 8P6, and Vene@8P6 at indicated points. (D, E) Representative image (D) and quantification (E) of γ-H2AX staining in THP-1 cells at 72 h after indicated treatments ($n = 50$ cells). Scale bar: 10 μm. (F, G) Representative image (F) and quantification (G) of γ-H2AX staining in HL60 cells at 72 h after indicated treatments ($n = 50$ cells). Scale bar: 10 μm. (H–M) Representative flow plots of ROS levels from THP-1 cells and HL60 cells. Representative flow plots of ROS levels from THP-1 cells (H) at 0, 24, 48, and 72 h after treatment Vene@8P6. Representative flow plots of ROS levels from THP-1 cells at 72 h after treatment with PBS, Vene, 8P6, Vene@8P6 (I, J). Representative flow plots of ROS levels from HL60 cells (K) at 0, 24, 48, and 72 h after treatment Vene@8P6. Representative flow plots of ROS levels from HL60 cells at 72 h after treatment with PBS, Vene, 8P6, Vene@8P6 (L, M). * $P < 0.05$, ** $P < 0.01$, *** $P < 0.001$, **** $P < 0.0001$. Data are presented as mean ± SD.

tively attacked leukemic cells which originally protected by residing in the bone marrow (BM) niche (Fig. 2J). Subsequently, we collected the bone marrow of AML mice administrated with DiL@8P6 and measured cell fluorescence to explore the cellular uptake and drug influence on cells (Fig. 2K). Twenty-four hours after DiL@8P6 administration *via* tail, we got a higher uptake rate from leukemia stem cells (LSCs) on account of 90.5%, and a relative high rate of 31.6% from AMLs. On the contrary, only 12.6% of T cells absorbed DiL@8P6. Besides, the uptake rate of most immune cells was less than 10%, expect NK cells and B cells but far less than LSCs (Figs. 2L and M). These results suggested that 8P6 precisely target LSC with little effect on other hematopoietic cells *in vivo*.

As 8P6 accurately targeted AML cells and spared hematopoietic cells and progenitors *in vivo*, we assumed that it might be applied for loading chemotherapeutic agents as a tool to avoid side effects and harm on other BM cells. Therefore, we encapsu-

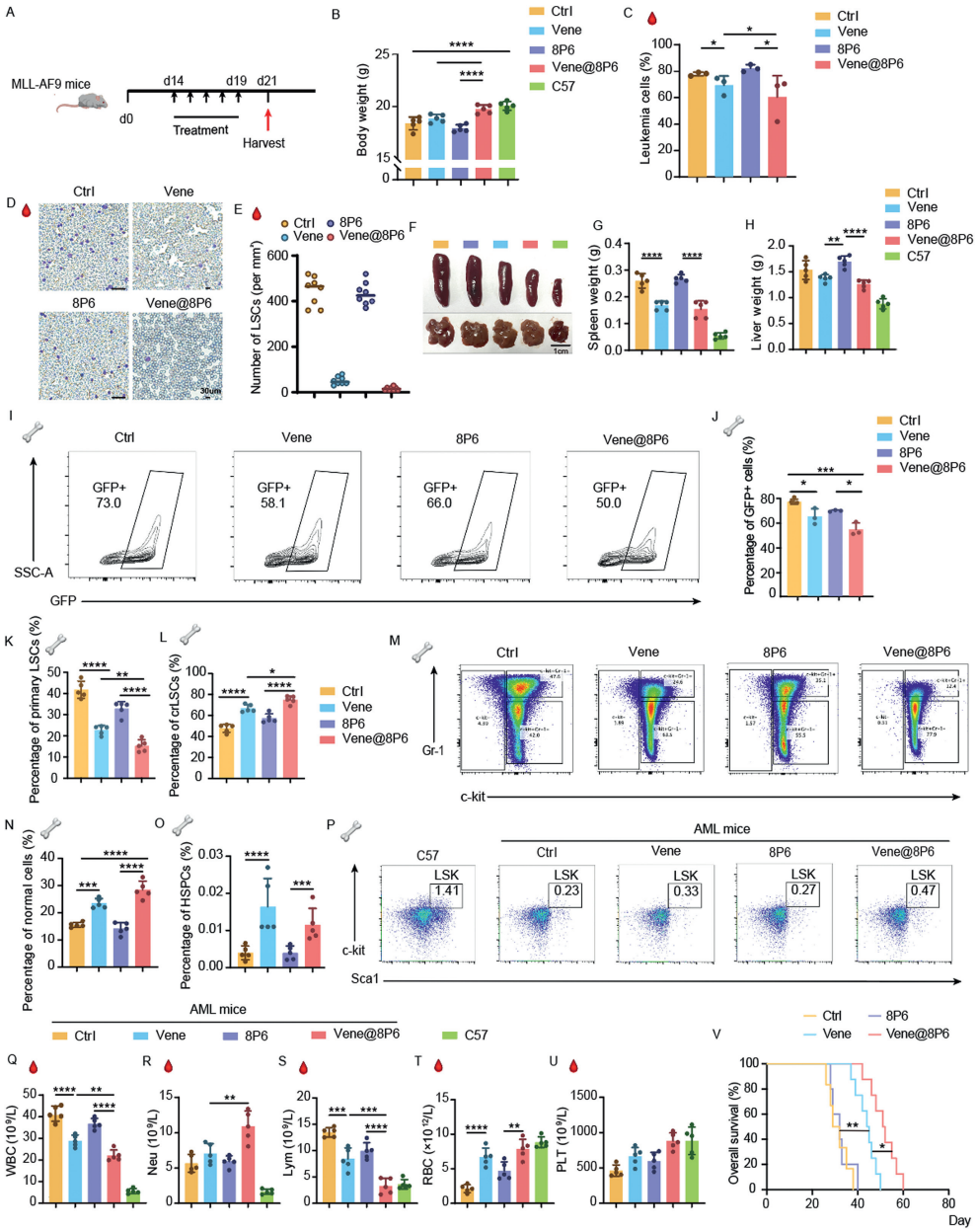

Fig. 4. Vene@8P6 has improved anti-leukemia effectiveness *in vivo*. (A) Treatment scheme for MLL-AF9 AML mice. (B) Body weight of MLL-AF9 mice for 21 days after transplantation with indicated treatment ($n = 5$ mice). (C) Frequency of MLL-AF9 cells of peripheral blood at the indicated time after treatments ($n = 5$ mice). Leukemia cells (GFP^+ cells). Cell morphology in a blood smear (D) and the percentage of GFP^+ leukemic cells of peripheral blood (E) of MLL-AF9 mice with the indicated treatment at 21 days after transplantation. Scale bar: 30 μm. Representative images (F) and weight quantification of liver (H) and spleen (G) of MLL-AF9 mice for 21 days after transplantation with indicated treatment ($n = 5$ mice). Percentage of GFP^+ cells (I, J), LSC (K–M), normal cells (N) and HSPC (O, P) in bone marrow of MLL-AF9 mice with the indicated treatment at 21 days after transplantation. (Q–U) Blood routine analysis of MLL-AF9 mice 21 days after transplantation with indicated treatment ($n = 5$ mice). (V) Overall survival of MLL-AF9 mice were analyzed after transplantation with indicated treatment. * $P < 0.05$, ** $P < 0.01$, *** $P < 0.001$, **** $P < 0.0001$. GFP: green fluorescent protein. Data are presented as mean ± SD.

lated 8P6 with Vene as Vene@8P6 to target leukemia cells. The proliferation of both THP-1 and HL60 was significantly inhibited on the influence of Vene@8P6 (Figs. 3A and C). Furthermore, it also increased the percentage of cell apoptosis in THP-1 dramatically in contract to free drug usage (Fig. 3B). Both THP-1 and HL60 cells revealed a significant decline of cell number on the proliferation administrated with Vene@8P6. Besides, while the proliferation of THP-1 cells in group of Vene@8P6 also significantly decreased compared with single drug therapy. Nanoparticles alone act less on cells. Moreover, we stained the two-style AML cells with γ-H_2AX *in vitro* to observe the DNA damage induced by the four types. Both fluorescence images and intensity analyses revealed that both 8P6 and Vene@8P6 caused severe DNA damage on THP-1 and HL60 cells (Figs. 3E and G). The relative intensity of γ-H_2AX of administration with Vene@8P6 examined by immunofluorescence staining was significantly severe than single chemotherapy drug (Figs. 3D and F). Considering the enhanced drug targeting and the consequent increase on leukemic cell damage above, we then stained the cells and detected reactive oxygen species (ROS) to analyze whether Vene@8P6 caused oxidative stress in leukemic cells. Nanoparticles with drug induced ROS more efficiently than free Vene in THP-1 and HL60 cells examined by fluorescence activating cell sorter (FACS) analysis for the ratio of ROS positive cells (Figs. 3H–M). Overall, we confirmed that Vene@8P6 triggered DNA

damage and apoptosis, induced by ROS by enhancing cellular uptake *in vitro*.

We next applied Vene@8P6 for AML treatment strategy to investigate the therapy. All animal experiments were performed based on protocols approved by the Institutional Animal Care and Use Committee or Ruiye Biotech Guangzhou Co., Ltd. Four treatments including phosphate buffered saline (PBS), 8P6, Vene and Vene@8P6 were respectively administrated with to MLL-AF9 AML mice *via* tail intravenous injection *in vivo* (Fig. 4A). Obviously, the two treatments with drugs rescued the AML mice weight. However, the weight of leukemia mice restored significantly after Vene@8P6 treatment, even approaching the weight of healthy C57BL/6J mice, whereas statistically different compared with the mice administered with drug (Fig. 4B). The percentage of leukemia cells of peripheral blood (PB) was down-regulated under Vene@8P6 in contrast to the other treatments, which indicated that nanoparticles with drug loading robustly reduced the leukemia burden (Fig. 4C). This result was also verified on blood smears and the related cell number count (Figs. 4D and E). Meanwhile, we also indicated that the size and weight of spleen and liver of AML mice (Figs. 4F–H), which recovered under Vene@8P6 treatment and attenuated the number of leukemia cells and LSCs in BM. The combination of chemotherapeutic agents and nanomaterials obviously enhanced the efficacy of Vene alone. Our previous study revealed a population of chemo-resistance LSCs (crLSCs), which are relevant to metabolic adaptations and preserved in a low ROS state. Compared with naive LSCs, crLSCs possess a slower cell cycle, activates immune evasion pathways and increases drug resistance exhibit distinct signatures [34]. CrLSCs is a subset of cells with drug resistance and tumor initiation functions. According to our BM flow cytometry results, primary LSCs treated with Vene@8P6 expressed significantly highly than that of the other three groups. Similar trends were observed on crLSCs (Figs. 4I–K). The flow cytometry results of leukemia cells in murine BM treated with the four administrations were demonstrated in (Figs. 4L and M). However, no significant difference was observed in hematopoietic stem and progenitor cells (HSPC) expression between the two groups with Vene and Vene@8P6, despite both were significantly higher than the other groups without drugs (Figs. 4N and O). In addition, in the presence of Vene@8P6 administered with AML mice *in vivo*, white blood cells and lymphocytes in the peripheral blood significantly declined while neutrophils, red blood cells and platelets increased (Figs. 4P–U). The effect of nanoparticle coated drugs is more efficiency than that of chemotherapy drugs alone. Ultimately, Vene@8P6 treatments significantly extended the mean overall survival to 60 days compared to the other treatment groups (Fig. 4V). The above results confirmed that nanoparticles embedding drugs targeted leukemia cells, relieved the symptoms of leukemia and improved the chemotherapy resistance *in vivo*.

Previous study has indicated that L-phenylalanine presented a maximum amount of absorption among amino acid molecule in mice [31]. Therefore, it may be the reason why L-phenylalanine targets leukemia cells while the underlying mechanisms requires exploration in further studies [31,35]. Amino acid polymers function as an effective leukemia-targeting drug carrier with high therapeutic effects for treatment [36]. Collectively, this study developed 8P6 as a novel nanocarrier based on L-phenylalanine of absorption and metabolism to inhibit LSCs and a precise drug delivery approach to target and treat AML.

Zheng *et al.* applied nanotechnology in macrophages on tumor immunotherapy and illustrated that nanoparticles are considered as promising carriers of tumor-associated macrophages (TAMs)-modulators by surface modification [37]. The treatment of hematological tumors is urgent, although Vene is extensively applied for chemotherapy in leukemia whereas accompanied by drug resistance [38], for common reasons including primary resistance that prognosis representing with highly heterogeneity, or acquired mutations in cancer-related genes such as BCL-2 that bind to Vene leading to highly reduced binding ability or subclonal metastasis [9,10,38-41]. Furthermore, dysregulation of BCL-2 family caused by changes in tumor microenvironment and mitochondrial changes in intracellular energy metabolism also trigger drug resistance [42,43]. Meanwhile, a series of intervention strategies also have been implemented. In our work, Vene coated with L-phenylalanine nanoparticles used as a drug delivery method to enhance the chemotherapy sensitivity from drug targeting, which improved the accuracy of Vene targeting and attacking leukemia cells with little side effect on hematopoietic normal cells.

Vene synergized with MCL-1 inhibitors, small molecule targeted drugs and other chemotherapeutic drugs targeting the tumor microenvironment effectively reduces the tumor adhesion, improves drug sensitivity, and increases the dependence of leukemia cells on BCL-2 anti-apoptotic pathway [12,44,45]. Albumin assembly and nanoparticle coating of sorafenib, another common chemotherapeutic agent applied in leukemia, mediates tumor reoxygenation and immune resensitization to enhance photodynamic immunotherapy [46]. And the combination of nigericin and decitabine wrapped with hexahistidine-metal nanocarriers also enabled to apply for pyroptosis-induced immunotherapeutics [47].

Besides, metabolic regulation with some drugs, combined immunochemotherapy and chimeric antigen receptor T-Cell immunotherapy (CAR-T) therapy are also applied to intervene Vene resistance [48-50]. This work is also consistent with previous work that Marian targets T-ALL *in vivo* and cysteine-based leukemia targeting nanocarrier loading paclitaxel (PTX) attacks AML [31,33]. We ultimately discovered that coated nanoparticles precisely targeted leukemia cells, retained normal hematopoietic function, and enhanced the anti-tumor ability of the AML mice. Furthermore, we obtained consistent results in corresponding *in vitro* experiments. In conclusion, we identified the targeting of Vene@8P6 in AML, and its treatment reduced the toxic side effects brought by Vene alone. Therefore, drug wrapped with nanoparticles can reduce body damage in leukemia chemotherapy and possesses high clinical application value.

Declaration of competing interest

The authors declare that they have no known competing financial interests or personal relationships that could have appeared to influence the work reported in this paper.

CRediT authorship contribution statement

Liangyu Zhang: Writing – review & editing, Writing – original draft, Validation. **Lei Lei:** Supervision, Data curation. **Zhuangzhuang Zhao:** Investigation, Formal analysis. **Guizhi Yang:** Formal analysis. **Kaitao Wang:** Supervision, Data curation. **Liying Wang:** Validation, Methodology, Data curation. **Ningxin Zhang:** Visualization, Investigation, Formal analysis. **Yanjia Ai:** Visualization, Validation. **Xinqing Ma:** Investigation, Formal analysis. **Guannan Liu:** Visualization, Validation. **Meng Zhao:** Writing – review & editing, Conceptualization. **Jun Wu:** Supervision, Resources, Methodology, Conceptualization. **Dongjun Lin:** Resources, Methodology, Conceptualization. **Chun Chen:** Supervision, Methodology.

Acknowledgments

We thank the National Natural Science Foundation of China (No. 52173150 to J. Wu), and the National Natural Science Foundation of China (No. 82370164 to C. Chen), Guangzhou Science and Technology Program City-University Joint Funding Project (No. 2023A03J0001 to J. Wu), the Affiliated Qingyuan Hospital of

Guangzhou Medical University Open Project Fund (No. 202301–211 to J. Wu), Sanming Project of Medicine in Shenzhen (No. SZSM201911004 to D. Lin and M. Zhao), National Natural Science Foundation of China (No. 92268205 to D. Lin), Doctoral Scientific Research Foundation of Changzhi Medical College, China (to Z. Zhao) and Post-doctoral Science Foundation (No. 2022M723670 to L. Wang) for supporting the manuscript preparation and publication.

Supplementary materials

Supplementary material associated with this article can be found, in the online version, at doi:10.1016/j.cclet.2024.110316.

References

[1] A. Khwaja, M. Bjorkholm, R.E. Gale, et al., Nat. Rev. Dis. Primers 2 (2016) 16010.
[2] H. Fan, F. Wang, A. Zeng, et al., Commun. Biol. 6 (2023) 765.
[3] H. Kantarjian, T. Kadia, C. DiNardo, et al., Blood Cancer J. 11 (2021) 41.
[4] C.T. Jani, A. Ahmed, H. Singh, et al., JCO Glob. Oncol. 9 (2023) e2300229.
[5] M. Mozaffari Jovein, G. Ihorst, J. Duque-Afonso, et al., Blood Cancer J. 13 (2023) 179.
[6] M. Pfirrmann, M. Baccarani, S. Saussele, et al., Leukemia 30 (2016) 48–56.
[7] M.S. Linet, R.E. Curtis, S.J. Schonfeld, et al., EClinicalMedicine 71 (2024) 102549.
[8] Y. Abaza, C. McMahon, J.S. Garcia, Am. Soc. Clin. Oncol. Educ. Book 44 (2024) e438662.
[9] R.W. Birkinshaw, J.N. Gong, et al., Nat. Commun. 10 (2019) 2385.
[10] A. Roca-Portoles, G. Rodriguez-Blanco, D. Sumpton, et al., Cell Death Dis. 11 (2020) 616.
[11] G.P. Sullivan, L. Flanagan, D.A. Rodrigues, T.N. Chonghaile, Sci. Transl. Med. 14 (2022) 674.
[12] Q. Zhang, B. Riley-Gillis, L. Han, et al., Signal Transduct. Target. Ther. 7 (2022) 51.
[13] B.A. Jonas, D.A. Pollyea, Leukemia 33 (2019) 2795–2804.
[14] B. Samra, M. Konopleva, A. Isidori, N. Daver, C. DiNardo, Front. Oncol. 10 (2020) 562558.
[15] K. Zhang, X. Zhang, Y. Xu, et al., Blood Cancer J. 13 (2023) 155.
[16] D.A. Pollyea, B.M. Stevens, C.L. Jones, et al., Nat. Med. 24 (2018) 1859.
[17] S.H. Chen, C.H. Jin, R. Ohgaki, et al., Sci. Rep. 14 (2024) 4651.
[18] K. Weidenauer, C. Schmidt, C. Rohde, et al., Leukemia 37 (2023) 1611–1625.
[19] R. Singh Mali, Q. Zhang, R.A. DeFilippis, et al., Haematologica 106 (2021) 1034–1046.
[20] R. Kawakatsu, K. Tadagaki, K. Yamasaki, et al., Sci. Rep. 14 (2024) 4975.
[21] R. Vazquez, C. Breal, L. Zalmai, et al., Blood Cancer J. 11 (2021) 62.
[22] K.W. Pratz, A.H. Wei, D.A. Pollyea, et al., Blood 134 (2019) 3897.
[23] S. Manda, B. Anziii, C. Benton, et al., Blood 138 (2021) 1265.
[24] M.G. Vander Heiden, Nat. Rev. Drug Discov. 10 (2011) 671–684.
[25] J. Chen, L. Cui, S. Lu, S. Xu, Cell Death Dis. 15 (2024) 42.
[26] Y. Tao, C. Dai, Z. Xie, et al., Chin. Chem. Lett. 35 (2024) 109170.
[27] Y. Wang, C. Zhang, S. Han, et al., Chin. Chem. Lett. 35 (2024) 109578.
[28] X. Li, R. Yue, G. Guan, et al., Exploration 3 (2023) 20220002.
[29] J. Sun, J. Li, X. Li, et al., Chin. Chem. Lett. 34 (2023) 107891.
[30] Z.N. Ling, Y.F. Jiang, J.N. Ru, et al., Signal Transduct. Target. Ther. 8 (2023) 345.
[31] C.Z. Li, X.R. You, X. Xu, et al., Adv. Sci. 9 (2022) 2104134.
[32] C. Xie, X. You, H. Zhang, Adv, et al., Adv. Sci. 10 (2023) e2300418.
[33] Y. Yu, Y. Meng, X. Xu, et al., ACS Nano 17 (2023) 3334–3345.
[34] X. Xu, Y. Yu, W. Zhang, et al., Nat. Cell Biol. 26 (2024) 464–477.
[35] B.M. Stevens, C.L. Jones, D.A. Pollyea, et al., Nat. Cancer 1 (2020) 1176–1187.
[36] H. Lemos, L. Huang, G.C. Prendergast, A.L. Mellor, Nat. Rev. Cancer 19 (2019) 162–175.
[37] Y. Zheng, Y. Han, Q. Sun, Z. Li, Exploration 2 (2022) 20210166.
[38] T.C. Teh, N.Y. Nguyen, D.M. Moujalled, et al., Leukemia 32 (2018) 303–312.
[39] C.D. DiNardo, M.Y. Konopleva, Nat. Cancer 2 (2021) 3–5.
[40] I. Kapoor, J. Bodo, B.T. Hill, et al., Cell Death Dis. 11 (2020) 941.
[41] Y. Nishida, J. Ishizawa, E. Ayoub, et al., Sci. Adv. 9 (2023) eadh1436.
[42] C.F.A. Warren, M.W. Wong-Brown, N.A. Bowden, et al., Cell Death Dis. 10 (2019) 177.
[43] R.J. Youle, A. Strasser, Nat. Rev. Mol. Cell Biol. 9 (2008) 47–59.
[44] Q. Zhang, L.N. Han, C. Shi, et al., Blood 128 (2016) 101.
[45] H. Widden, W.J. Placzek, Commun. Biol. 4 (2021) 1029.
[46] Z. Zhou, J. Chen, Y. Liu, et al., Acta Pharma. Sin. B 12 (2022) 4204–4223.
[47] Q. Niu, Y. Liu, Y. Zheng, et al., Acta Pharma. Sin. B 12 (2022) 4458–4471.
[48] S.J. McPhedran, G.A. Carleton, J.J. Lum, et al., Nat. Metab. 6 (2024) 396–408.
[49] K. Keijzer, J.W. de Boer, J.A. van Doesum, et al., Blood Cancer J. 14 (2024) 41.
[50] J.J. Peng, L. Wang, Z. Li, et al., Sci. Immunol. 8 (2023) eabq3016.